Spectroscopy Letters

ISSN: 0038-7010 (Print) 1532-2289 (Online) Journal homepage: http://www.tandfonline.com/loi/lstl20

Spectroscopy, Electrochemistry, and Structure of 3d-Transition Metal Complexes of Thiosemicarbazones with Quinoline Core: Evaluation of Antimicrobial Property

Naveen V. Kulkarni , Ganesh S. Hegde , Gurunath S. Kurdekar , Srinivasa Budagumpi , M. P. Sathisha & Vidyanand K. Revankar

To cite this article: Naveen V. Kulkarni , Ganesh S. Hegde , Gurunath S. Kurdekar , Srinivasa Budagumpi , M. P. Sathisha & Vidyanand K. Revankar (2010) Spectroscopy, Electrochemistry, and Structure of 3d-Transition Metal Complexes of Thiosemicarbazones with Quinoline Core: Evaluation of Antimicrobial Property, Spectroscopy Letters, 43:3, 235-246, DOI: 10.1080/00387010903329383

To link to this article: https://doi.org/10.1080/00387010903329383

Published online: 05 Apr 2010.

Spectroscopy Letters, 43:235–246, 2010

ISSN: 0038-7010 print/1532-2289 online
DOI: 10.1080/00387010903329383

Taylor & Francis
Taylor & Francis Group

Spectroscopy, Electrochemistry, and Structure of 3d-Transition Metal Complexes of Thiosemicarbazones with Quinoline Core: Evaluation of Antimicrobial Property

Naveen V. Kulkarni, Ganesh S. Hegde, Gurunath S. Kurdekar, Srinivasa Budagumpi, M. P. Sathisha, and Vidyanand K. Revankar

Department of Studies in Chemistry, Karnatak University, Pavatenagar, Dharwad, Karnataka, India

ABSTRACT A series of Co(II), Ni(II), Cu(II), and Zn(II) complexes of quinoline-thiosemicarbazones was prepared. The Schiff base ligands that provide N, O, and S donor atoms for ligation are synthesized by the condensation of 2-hydroxy-3-formylquinoline with substituted thiosemicarbazides in ethanol. The ligands and complexes are characterized by elemental analysis, infrared, ^{1}H NMR, UV-Vis, fast atom bombardment (FAB) mass spectroscopy, and electron spin resonance (ESR) spectral studies followed by magnetic susceptibility and conductivity measurements. The ligand-to-metal ratio is found to be 1:1 and 2:2 for the complexes of L^1H_2 and L^2H_2, respectively. All the complexes are found to have octahedral geometry except $[CuL^1H(H_2O)Cl]$, which exhibits a square pyramidal structure. All the complexes are nonelectrolytic in nature and the electrochemical behavior of complexes is dealt with briefly. Further ligands and complexes were evaluated for their antimicrobial activity against bacteria *Escherichia coli* and *Pseudomonas aeruginosa* and fungi *Aspergillus niger and Cladosporidium*.

KEYWORDS antimicrobial activity, electrochemistry, quinoline, thiosemicarbazone

INTRODUCTION

Thiosemicarbazones are an important class among the sulfur-containing compounds, in view of their versatility in the coordination behavior and pharmacological applications. Thiosemicarbazones and their metal complexes are well known for their anticarcinogenic, antibacterial, and antifungal properties.[1,2] It has been shown in the literature that the metal derivatives are more effective than the free ligands in anticancer activity. One of the many reasons is that the binding affinity of metals to proteins or enzymes will change the interaction process with DNA, thereby affecting DNA replication and cell proliferation.[3] In this context, hybrid chelate ligands containing mixed functionalities are widely used as ligands for the isolation of interesting and important metal complexes.[4] In particular,

Received 23 July 2009;
accepted 11 September 2009.

Address correspondence to Vidyanand K. Revankar, Department of Studies in Chemistry, Karnatak University, Pavatenagar, Dharwad-580 003, Karnataka, India.
E-mail: vkrevankar@rediffmail.com

thiosemicarbazone usually coordinates metal ions through the imine nitrogen and the sulfur atom in a bidentate mode and can increase the coordination mode to tridentate with incorporation of additional donor groups as heterocyclic substituents. The most popular donor set involves ONS or NNS atoms displaying versatile coordination behavior like monomers, with one or two ligands attached to the metal ion, or dimers, in which the metal centers can be bridged through either the thiolate sulfur or the non-thiosemicarbazone coligand (i.e., Cl, N_3, NCS, CH_3COO, etc.).[5] Biological studies have shown that the type of substitution influences the antimicrobial effects and enhancement of the biological activity of the complexes.[6] Quinoline, the backbone for most natural products, is used for the design of many synthetic compounds having diverse pharmacological applications such as antibacterial, antifungal,[7] immunosuppressive,[8] analgesic, vasorelaxing,[9] antiplasmodial,[10] anticancer,[11] anticonvulsant, and antihypertensive[12] activities. Further quinoline core incorporation with appropriate functional groups can serve as a precursor for the synthesis of potential ligands. In this context, we have designed new ligand systems in which 3-hydroxy-3-formyl quinoline was introduced into the backbone of thiosemicarbazone or vice versa to further investigate the chemistry of a new quinoline-thiosemicarbazones and their metal derivatives and to investigate their potential usefulness as therapeutic agents.

MATERIALS AND METHODS

The chemicals used were of reagent grade. Purified solvents were used for the synthesis of ligands and complexes. Synthesis of 2-chloro-3-formyl quinoline was carried out according to the reported method with slight modification,[13] which on acid hydrolysis yields 3-hydroxy-3-formyl quinoline. Thiosemicarbazides were prepared by the method described in the literature.[14] The metal chlorides used were in the hydrated form. C, H, N, and S analysis was carried out on a Thermo Quest elemental analyzer (Milan, Italy). Metal and chloride estimations were done following standard procedures. The molar conductivity measurements in dimethylformamide (DMF) were made on an ELICO-CM-82 conductivity bridge (EITI Ltd., Hyderabad, India) with a conductivity cell having a cell constant 0.51 cm^{-1}. The magnetic susceptibility measurements were made using a Faraday balance at room temperature using $Hg[Co(SCN)_4]$ as a calibrant. The ^1H NMR spectra were recorded in DMSO-d_6 solvent on a Bruker 300-MHz spectrometer (USA) at room temperature using tetramethylsilane (TMS) as internal reference. Infrared (IR) spectra were recorded in KBr matrix using an Impact 410 Nicolet Fourier transform infrared (FTIR) spectrometer (USA) in the 4000–400 cm^{-1} range. The electronic spectra of the complexes were recorded on a Hitachi 150-20 in the spectrophotometer in range 1000–200 nm. Cyclic voltammetric studies were performed at room temperature in DMF under oxygen free condition created by purging pure nitrogen gas, with a CHI1110A electrochemical analyzer (USA) comprising a three-electrode assembly of glassy carbon working electrode, platinum auxiliary electrode, and Ag/AgCl reference electrode. Tetramethylammonium chloride (0.01 M) was used as supporting electrolyte and the instrument was standardized by a ferrocene/ferrocenium redox couple. The ESR study of the copper complexes was carried out on a Varian E-4X-band electron paramagnetic resonance (EPR) spectrometer (USA), using tetracyanoethylene (TCNE) as the g-marker. Fast atom bombardment (FAB) mass spectra were recorded on a JEOL SX102/DA-6000 mass spectrometer (Tokyo, Japan) using argon/xenon (6 kV, 10 mA) as the FAB gas and m-nitro-benzyl alcohol the as matrix.

Synthesis of Thiosemicarbazones

Thiosemicarbazide (0.01 mol) in ethanol (100 mL) was treated with 2-hydroxy-3-formyl quinoline (0.01 mol). The reaction mixture was refluxed for 3–4 hr and the yellow solid separated was filtered, washed two to three times with ethanol, and dried (Scheme 1).

Synthesis of Complexes

Ligand (0.001 mol) was taken in 35–40 mL of hot ethanol. To this, a hot ethanolic solution of metal

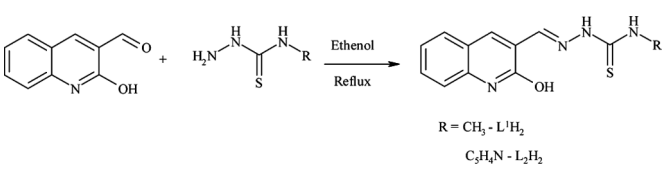

SCHEME 1 **Reaction pathway representing the preparation of thiosemicarbazones.**

chloride (0.001 mol) was added drop-wise with stirring at 60–65°C. After complete addition of metal salt solution, the reaction mixture was stirred for another 30–40 min at the same temperature and refluxed for 3–4 hr in a water bath. The isolated complexes were filtered in hot condition, washed with hot ethanol, and dried.

Antibiogram Analysis of Compounds against Bacteria

Media used in the analysis was prepared by adding 10 g of peptone and 10 g of sodium chloride to the homogeneous mixture of 5 g of yeast extract and 20 g of nutrient agar taken in 1000 mL of distilled water. Initially, the stock cultures of *Escherischia coli* and *Pseudomonas aeruginosa* were revived by inoculating in broth media and grown at 37°C for 18 hr. The agar plates of the above media were prepared and wells were made in the plate. Each plate was inoculated with 150 μL of 18-hr-old cultures and spread evenly on the plate. After 20 min, the wells were filled with 100 μL of each compound (10 mg/mL in DMF). The control plates with gentamycin (10 mg/mL) and DMF were also prepared. All the plates were incubated at 37°C for 24 hr and the diameters of inhibition zone were noted in centimeters. The values were compared with that of gentamycin and the samples showing significant inhibition were selected for the further calculation of minimum inhibition concentration (MIC). The MICs of compounds were determined by assaying at 500 and 250 μg concentrations along with standard gentamycin at the same concentrations. The cultures were grown for 24 hr and the zones were compared with that of gentamycin and percentage of inhibition was calculated.

Antibiogram Analysis of Compounds against Fungi

Potato dextrose agar (PDA) media used in the analysis was prepared by mixing 20 g of dextrose to the filtrate obtained by the 250 g of peeled potato boiled for 20 min, squeezed, and filtered; the volume was made up to 1000 mL by adding distilled water.

Initially, the stock cultures of *Aspergillus niger* and *Cladosporidium* were revived by inoculating in broth media and grown at 37°C for 48 hr. The agar plates of the above media were prepared and wells were made in the plate. Each plate was inoculated with 150 μL of 48-hr-old cultures and spread evenly on the plate. After 20 min, the wells were filled with 500 μL of each compound (10 mg/mL in DMF). Control plates with fluconazole (10 mg/mL) and DMF were also prepared. All plates were incubated at 37°C for 48 hr and the diameters of the inhibition zone were noted in centimeters. The values were compared with that of fluconazole and the samples showing significant inhibition were selected for further calculation of MIC.

The MICs of compounds were determined by assaying at 500- and 250-μg concentrations along with standard fluconazole at the same concentrations. The cultures were grown for 48 hr and the zones were compared with that of fluconazole and percentages of inhibition were calculated.

RESULTS AND DISCUSSION

The complexes obtained in the present study were nonhygroscopic and in the form of amorphous solids. The metal complexes are easily soluble in DMSO and DMF and sparingly soluble in ethanol and methanol, whereas they are insoluble in chlorinated hydrocarbons. The metal complexes melt with decomposition above 300°C. The elemental analysis data of the ligands and their complexes along with molar conductivity values are compiled in Table 1.

Molar Conductivity Measurements

The molar conductance values of the complexes measured at room temperature in DMF solution with 10^{-3} mol/dm^3 concentration fall in the range 4.6 to 8.9 ohm^{-1} cm^2 mol^{-1}, indicating the nonelectrolytic nature of the complexes.

IR Spectral Studies

Important IR absorption bands are summarized in Table 2. The possibility of thione-thiol tautomerism (H−N−C=S ⇔ C=N−SH) in the ligands has been ruled out, because there is no band around 2500–2600 cm^{-1}, which is characteristic of a thiol group. The amine $\upsilon(^4\text{NH})$ and hydrazine $\upsilon(^2\text{NH})$ are observed around 3300 and 3150 cm^{-1}, respectively. Coupled vibration among the components of thioamide bands I [υ(CN) and β(NH) + δ(CH)], II [υ(CN) and β(CS)], III [υ(CS) and υ(CS) + υ(CN)], and IV

TABLE 1 Elemental Analysis and Molar Conductivity Data

Compound	Elemental analysis (%) calculated (found)						Molar cond. ΛM ($ohm^{-1}\ cm^2\ mol^{-1}$)
	C	H	N	S	M	Cl	
L^1H_2	55.38 (55.62)	4.62 (4.93)	21.83 (21.76)	12.30 (12.48)	—	—	4.6
$[CoL^1H(H_2O)_2Cl]\cdot 2H_2O$	33.89 (34.02)	4.38 (4.30)	13.16 (13.21)	7.46 (7.54)	13.86 (14.02)	8.12 (8.21)	6.8
$[NiL^1H(H_2O)_2Cl]\cdot 2H_2O$	33.92 (34.11)	4.44 (4.51)	13.13 (13.18)	7.53 (7.58)	13.78 (13.98)	8.24 (8.32)	5.3
$[CuL^1H(H_2O)Cl]$	38.40 (38.86)	3.46 (3.51)	14.93 (14.80)	8.53 (8.48)	16.93 (17.02)	9.33 (9.25)	8.8
$[ZnL^1H(H_2O)_2Cl]\cdot H_2O$	34.82 (35.03)	4.11 (4.23)	13.54 (13.63)	7.73 (7.82)	15.84 (16.12)	8.46 (8.52)	7.3
L^2H_2	59.44 (59.62)	4.02 (4.13)	21.67 (21.76)	9.90 (10.02)	—	—	6.7
$[Co_2L^2_2(H_2O)_4]\cdot 2H_2O$	44.03 (44.14)	4.30 (4.38)	16.05 (16.13)	7.30 (7.62)	13.50 (13.83)	—	7.9
$[Ni_2L^2_2(H_2O)_4]\cdot 2H_2O$	44.00 (44.10)	4.36 (4.52)	16.00 (16.32)	7.34 (7.53)	13.43 (13.62)	—	8.9
$[Cu_2L^2_2(H_2O)_4]$	45.41 (45.56)	4.02 (4.23)	16.50 (16.43)	7.57 (7.73)	15.02 (15.13)	—	8.2
$[Zn_2L^2_2(H_2O)_4]\cdot H_2O$	44.21 (44.54)	4.15 (4.23)	16.14 (16.26)	7.38 (7.58)	15.10 (15.27)	—	5.2

[υ(CS)] are distributed around 1590, 1490, 1430, and 950 cm^{-1}. The quinoline υ(OH) is found around 3050 cm^{-1} as a weak band that disappears in all complexes, indicating deprotonation and coordination to metal. This is further supported by a shift of υ(C−O) to a higher frequency.[15] Thioamide bands III and IV, which have major contribution of υ(C=S), have undergone considerable reduction in intensity and shifted to lower frequency in the complexes of L^1H_2, indicating the involvement of thione sulfur in the coordination. Further, in all other complexes these bands remain absent, suggesting the thioenolization and subsequent coordination to the metal, which is supported by the appearance of a weak band around 600–650 cm^{-1} due to υ(C−S) and disappearance of $\upsilon(^2N-H)$. The band due to $\upsilon(^4NH)$ remains unaltered in all the complexes and the broad band observed around 3400 cm^{-1} is assigned to υ(OH) of water molecule. The band around 1633–1655 cm^{-1}, which is assigned to υ(C=N), has shifted to lower energy, supporting the coordination of azomethine nitrogen. The low-frequency nonligand bands in the 515–450 cm^{-1} and 400–440 cm^{-1} region are assigned to υ(M−N) and υ(M−S), respectively.

^{1}H NMR Studies

In the ^{1}H NMR spectra of ligands a sharp singlet observed around 12.06 ppm attributable to the hydroxy group of quinoline disappeared in the zinc complexes, indicating the deprotonation followed by the coordination of oxygen. The azomethine protons experience the downfield shift in $[ZnL^1H(H_2O)_2Cl]\cdot H_2O$ and upfield shift in $[Zn_2L^2_2(H_2O)_4]\cdot H_2O$, indicating the coordination of azomethine group to the metal center. The presence of a peak assignable to the hydrazine −NH in the spectrum of $[ZnL^1H(H_2O)_2Cl]\cdot H_2O$ with a slightly different δ value than the ligand suggests the thione form of ligand in the complex. In case of zinc complex of L^2H_2, no peak with respect to hydrazine −NH was observed, suggesting the thiol form of ligand and ligation of sulfur upon deprotonation. The aromatic protons distributed in the range 6–8 ppm of spectra of free ligands show small shifts in complexes that are attributable to a variation in electron density and steric constraints brought about by chelation. The presence of coordinated water molecules is evidenced by the peak observed around 3.60 ppm in the spectra. It overlaps with the DMSO peak at 3.50 ppm and broadens the signal. The numerical NMR data are given in Table 3 and the spectra of L^1H_2 and $[ZnL^1H(H_2O)_2Cl]\cdot H_2O$ are given in Fig. 1.

Electronic Spectral Studies

Both ligands exhibit similar electronic transitions with bands around 260–300 nm, assigned to the intraligand $\pi \rightarrow \pi^*$ transition, which were almost unchanged in the spectra of complexes. A broad band at ~390 nm with a shoulder on the low energy side is observed due to $n \rightarrow \pi^*$ transition associated with azomethine linkage. This band suffers a red shift in all complexes due to participation of azomethine nitrogen in coordination. The band observed near 415 nm in the complexes with $\varepsilon \sim 25{,}000$ l cm^{-1} mol^{-1} is assigned to S → M (LMCT).[15a,b] Electronic spectra of cobalt complexes show d-d transitions

TABLE 2 **Infrared Spectral Data of Ligands and Complexes in cm^{-1}**

Compound	ν (OH) water	ν (^{4}NH)	ν (^{2}NH)	ν (C=N)	Thioamide bands I	II	III	IV	ν (O−H) quinoline	ν (N−N)	ν (C−S)	ν (C−O)	β(OH)	ν (M−N)	ν (M−S)
L^1H_2	—	3343	3159	1655	1590	1528	1442	960	3062	1087	—	1255	1377	—	—
$[CoL^1H(H_2O)_2Cl]\cdot 2H_2O$	3392	3200	3135	1634	1601	1496	1435	933	—	1089	—	1265	—	500	430
$[NiL^1H(H_2O)_2Cl]\cdot 2H_2O$	3383	3191	3130	1641	1601	1496	1437	942	—	1085	—	1261	—	472	438
$[CuL^1H(H_2O)Cl]$	33432	3399	3185	1639	1602	1484	1434	952	—	1094	—	1263	—	501	428
$[ZnL^1H(H_2O)_2Cl]\cdot H_2O$	3416	3337	—	1643	1606	1477	1430	953	—	1095	—	1263	—	512	422
L^2H_2	—	3286	3216	1652	1607	1498	1433	931	3050	1081	—	1228	1371	—	—
$[Co_2L_2^3(H_2O)_4]\cdot 2H_2O$	3399	3200	3180	1633	1600	1470	—	—	—	1048	616	1267	—	461	412
$[Ni_2L_2^2(H_2O)_4]\cdot 2H_2O$	3412	—	3143	1636	1602	1479	—	—	—	—	607	1258	—	471	421
$[Cu_2L_2^2(H_2O)_4]$	3417	3200	3157	1647	1600	1472	—	—	—	1056	603	1256	—	462	416
$[Zn_2L_2^2(H_2O)_4]\cdot H_2O$	3426	—	3100	1645	1602	1482	—	—	—	1034	623	1231	—	470	418

TABLE 3 NMR Spectral Data

Compound	^{1}H NMR δ ppm						
	Ar−H	−HC=N	Quinoline OH	Hydrazine NH	R−NH	$-CH_3$	H_2O
H_2L^1	7.2–7.68	8.67	12.01	11.70	8.60	2.51	—
$[ZnL^1H(H_2O)_2Cl]\cdot H_2O$	6.9–7.89	8.70	—	11.6	8.4	2.50	3.60
H_2L^2	7.2–7.8	8.85	12.06	11.64	9.89	—	—
$[Zn_2L^2_2(H_2O)_4]\cdot H_2O$	6.9–7.8	8.55	—	—	8.0	—	3.50

around 580, 450, and 910 nm assignable to $^4T_{1g} \rightarrow {}^4A_{2g}$, $^4T_{1g}(F) \rightarrow {}^4T_{1g}(P)$, and $^4T_{1g}(F) \rightarrow {}^4T_{2g}$ transitions with a sharp charge transfer band at 410 nm, which is inconsistent with the octahedral geometry. In Ni(II) complexes the lowest energy band observed at 910 nm was due to $^3A_{2g} \rightarrow {}^3T_{2g}$ (ν_1) and bands near 650 and 450 nm were assigned to $^3A_{2g} \rightarrow {}^3T_{1g}$ (ν_2) and $^3A_{2g} \rightarrow {}^3T_{1g}$ (P) (ν_3), respectively. Appearance of these three spin allowed d-d bands assigns octahedral geometry around the Ni ion.[16] In case of $[CuL^1H(H_2O)Cl]$ the low energy asymmetric band observed at 550 nm was assigned to d-d transition. A similar type of the bands with low energy shoulder band were assigned for Schiff base Cu(II) complexes with square pyramidal geometry.[17] $[Cu_2L^2_2(H_2O)_4]$ exhibits absorptions around 500 and 650 nm with low ε value. Generally Cu(II) ions can adopt square-planar, square-pyramidal, trigonal-bipyramidal,

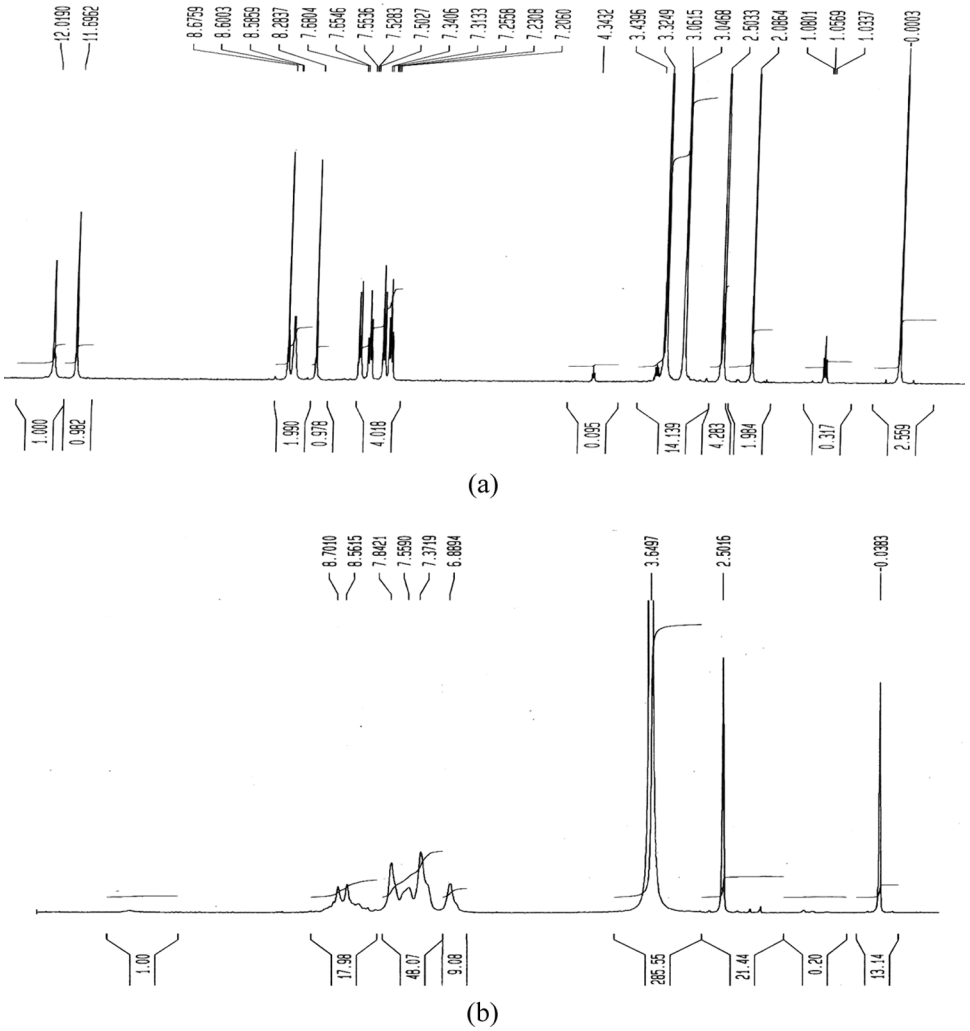

FIGURE 1 ^{1}H NMR spectra. (a) ^{1}H spectrum of L^1H_2. (b) ^{1}H spectrum of L^1HZn.

octahedral, and tetrahedral geometries, which, except for the first, are generally distorted from the idealized structures. The d-d spectra shown by these coordination geometries are distinctive only in the case of the tetrahedral environment where the absorptions occur at much lower energies and generally show well-separated absorption peaks; in case of all other distorted geometries, the spectrum shows closely spaced absorption manifolds. Hence, it is difficult to predict the accurate structure for the complexes only on the basis of electronic spectral analysis. Zn(II) complexes show only the absorptions around 400 and 420 nm, which corresponds to intraligand transitions. The electronic spectral data of the ligands and their complexes are summarized in Table 4 and the spectra of L^2H_2 and $[Ni_2L_2^2(H_2O)_4]\cdot 2H_2O$ are given in Fig. 2.

EPR Studies

The solid-state X-band EPR spectra of copper complexes of L^1H_2 and L^2H_2 exhibit isotropic intense broad signals with g_{iso} values 2.09 and 2.05, respectively, with no hyperfine splitting in $g_{\parallel}$ or $g_{\perp}$ region. No half-field absorption, which is an index of metal–metal interaction, was observed. This type of spectra was reported earlier for the complexes bearing large organic ligand substituents having considerable covalent character for metal–ligand bonds.[18a] The low g_{iso} values are attributed to the presence of sulfur coordination in the complexes. A similar comparison is made between S-bonded and O-bonded complexes. A decrease of 0.144 in g_{eff} values for S-bonded complexes was observed when compared with the O-bonded complexes. It is concluded that the EPR parameters are dependent on the coordinating atoms. This type of behavior has been observed for Schiff base complexes and is attributed to (a) higher covalancy of Cu−S compared to Cu−O bond and (b) higher spin–orbit coupling constants for sulfur than for oxygen. Both factors reduce the spin–orbit contribution of the Cu(II) ion to the g-tensor, decreasing the g-value.[18b] We observe here that the complex $[Cu_2L^2(H_2O)]$, which has two thiolate sulfur atoms bridging between the two metal centers, possesses lower g_{iso} value (2.05) compared to the complex $[Cu_2L_2^1Cl(H_2O)]$ ($g_{iso} = 2.09$), which has only one nonbridging sulfur coordination. This observation evidences the dependency of EPR parameters on the coordinating atoms. The presence of two bridging sulfur atoms in the former complex may lead a maximum reduction in the spin–orbit contribution of Cu(II) into the g-tensor, giving a lower g-value for the complex.

Magnetochemistry

The experimentally determined room temperature magnetic moments of all the complexes are given in the Table 4. The copper complexes of L_1H^2 and L_2H^2 exhibit the effective magnetic moment (μ_{eff}) of 1.58 and 1.40 BM at 303 K. Fairly lesser effective magnetic moment values are indicative of higher covalancy of Cu-S bond and lower order spin–orbit coupling of sulfur. The magnetic moment values of Ni(II) complexes give valuable information regarding their stereochemistry. This is due to favorable changes occurring in the number of unpaired electrons and the orbital contribution to the magnetic moments, when stereochemistry around the Ni(II) ion is changed. The octahedral complexes have $^3A_{2g}$ ground state and hence the orbital contribution to the

TABLE 4 Electronic Spectra and Magnetic Moment Data

Compound	λ_{max} (nm)	μ_{eff} (B.M)
L^1H_2	270, 341, 356, 366, 372, 391	—
$[CoL^1H(H_2O)_2Cl]\cdot 2H_2O$	321, 333, 348, 401, 450, 580, 912	4.31
$[NiL^1H(H_2O)_2Cl]\cdot 2H_2O$	303, 369, 414, 450, 688, 916	2.92
$[CuL^1H(H_2O)Cl]$	323, 350, 403, 450, 550	1.58
$[ZnL^1H(H_2O)_2Cl]\cdot H_2O$	280, 353, 401, 420	Diamagnetic
L^2H_2	268, 288, 318, 357, 393	—
$[Co_2L_2^2(H_2O)_4]\cdot 2H_2O$	347, 371, 435, 500, 913	4.35
$[Ni_2L_2^2(H_2O)_4]\cdot 2H_2O$	321, 336, 414, 450, 680, 916	2.81
$[Cu_2L_2^2(H_2O)_4]$	300, 369, 420, 500, 650	1.40
$[Zn_2L_2^2(H_2O)_4]\cdot H_2O$	340, 370, 421	Diamagnetic

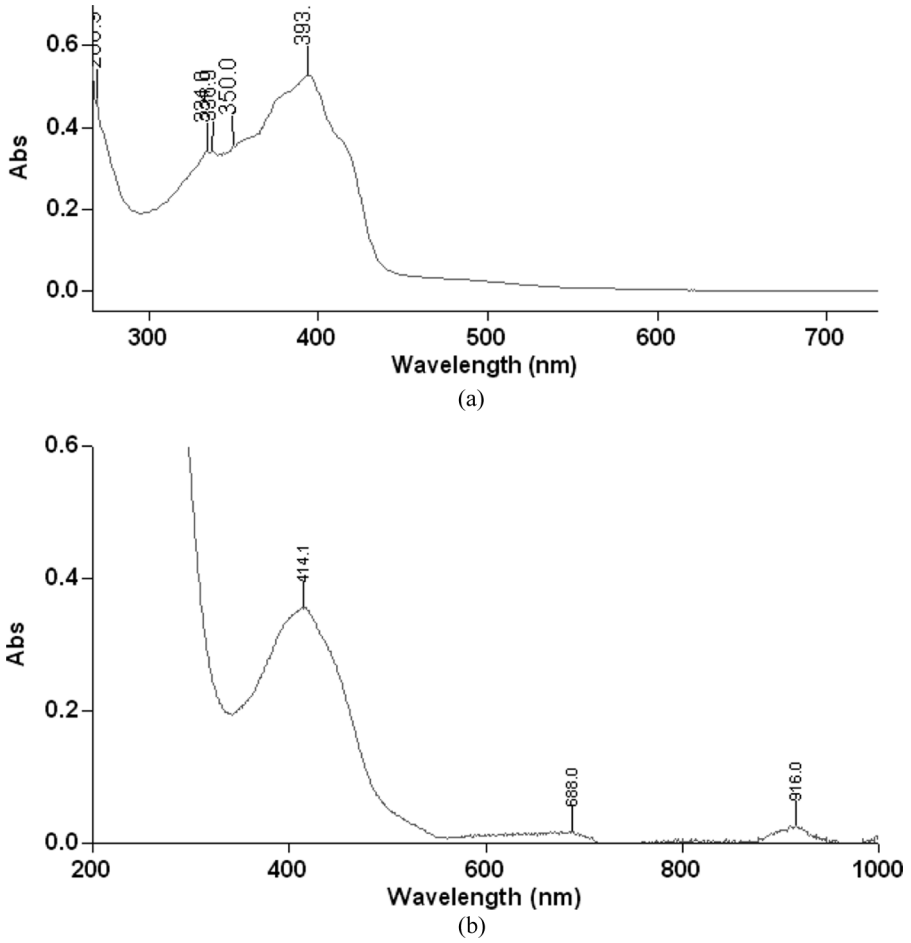

FIGURE 2 **The electronic spectra of ligand and complex. (a) Electronic spectrum of L^2H_2. (b) Electronic spectrum of $[Ni_2L_2^2(H_2O)_4]\cdot 2H_2O$.**

magnetic moment due to orbital degeneracy is absent. However, octahedral nickel(II) complexes show the effective magnetic moments that are more than the spin-only value of 2.83 B.M. This is because the excited state $^3T_{2g}$ carries the orbital magnetic moment. The spin–orbit coupling brings about some mixing of the ground state with the excited state, thus forcing some orbital contribution that increases the magnetic moment for about 10% than the spin-only value. Therefore, magnetic moment values obtained in the present investigation, 2.92 and 2.81, indicate an octahedral geometry around the nickel(II) ion for both complexes.[19] The cobalt complexes exhibit paramagnetic susceptibility, with corresponding magnetic moment values lying around 4.30–4.35 BM, which signify the octahedral geometry. The subnormal magnetic moment values are accounted for the higher covalancy of Cu-S bond and lower order spin–orbit coupling of sulfur.[20]

Mass Spectral Analysis

The elemental and analytical data suggest the empirical formula $[CuL^1H(H_2O)Cl]$ and $[Cu_2L_2^2(H_2O)_4]$ for both the copper complexes, respectively, which is supported by the FAB mass spectral analysis. The peaks at highest m/z value can be assigned to the molecular ion by certainty, with the aid of a consistent isotopic pattern. A peak observed at m/z 378 for the $[CuL^1H(H_2O)Cl]$ complex is in consistent with the molecular mass of the complex, representing the monomeric structure. The FAB mass spectrum of $[Cu_2L_2^2(H_2O)_4]$ exhibits a molecular ion peak at m/z 841, which evidences the proposed binuclear structure of complex. Apart from this, the mass spectra show some other peaks, which are due to molecular cations of various fragments of the complex. By comparing the analytical and spectral data of cobalt, nickel, and zinc complexes, similar structures were assigned for the respective

series. The proposed structures assigned are represented in Fig. 3.

Electrochemistry

The cyclic voltammograms (CV) of all ligands and their complexes were scanned in the potential range of +1.0 to −1.0 V with different scan rates (0.15, 0.1, and 0.05 V/s). Both the copper complexes exhibit a redox property, whereas ligands and other complexes do not show any electrochemical response over the working potential range, indicating that electrochemical activity of the copper complexes is purely metal based. The voltammograms of the two copper complexes are illustrated in Fig. 4 and numerical results are compiled in Table 5. The voltammogram of $[Cu_2L^2_2(H_2O)_2]$ shows a single oxidation peak in the range 0.43–0.46 V in the anodic potential scan. The cathodic scan exhibits a single peak in the range 0.32–0.35 V, indicating the reduction of species. The high value of ΔE_p, separation between the cathodic and anodic peak potentials ($E_{pa} - E_{pc}$), which is greater than 60 mV, indicates quasi-reversible redox process[21] assignable to the Cu(III)/Cu(II) couple with $E_{1/2}$ $[(E_{pc} + E_{pa})/2]$ value ∼0.39 V. The appearance of Cu(III)/Cu(II) and absence of Cu(II)/Cu(I) couple can be rationalized in terms of flexibility and the size of the coordination cavity in the complexes and the geometric requirements and the size of the metal ions in the different oxidation states. The voltammogram of complex $[CuL^1Cl(H_2O)]$ exhibits one irreversible cathodic (reduction) peak in the range −0.23 to −0.28 V along with quasi-reversible reaction peaks (with E_{pa} in the range 0.11–0.13 V and E_{pc} 0.18–0.23) assigned to Cu^{III}/Cu^{II} couple, with the I_{pc}/I_{pa} ∼1. A voltammogram of complexes scanned after keeping the solution overnight and at slower rates shows a decrease in ΔE_p value, indicating the reversibility of reaction with a slow rate.

Antimicrobial Analysis of the Compounds

The prepared ligands, Cu(II) and Ni(II) complexes, were screened for antimicrobial activity against bacteria *Escherichia coli* and *Pseudomonas aeruginosa* and fungi *Aspergillus niger* and *Cladosporidium*. The results obtained are graphically represented in

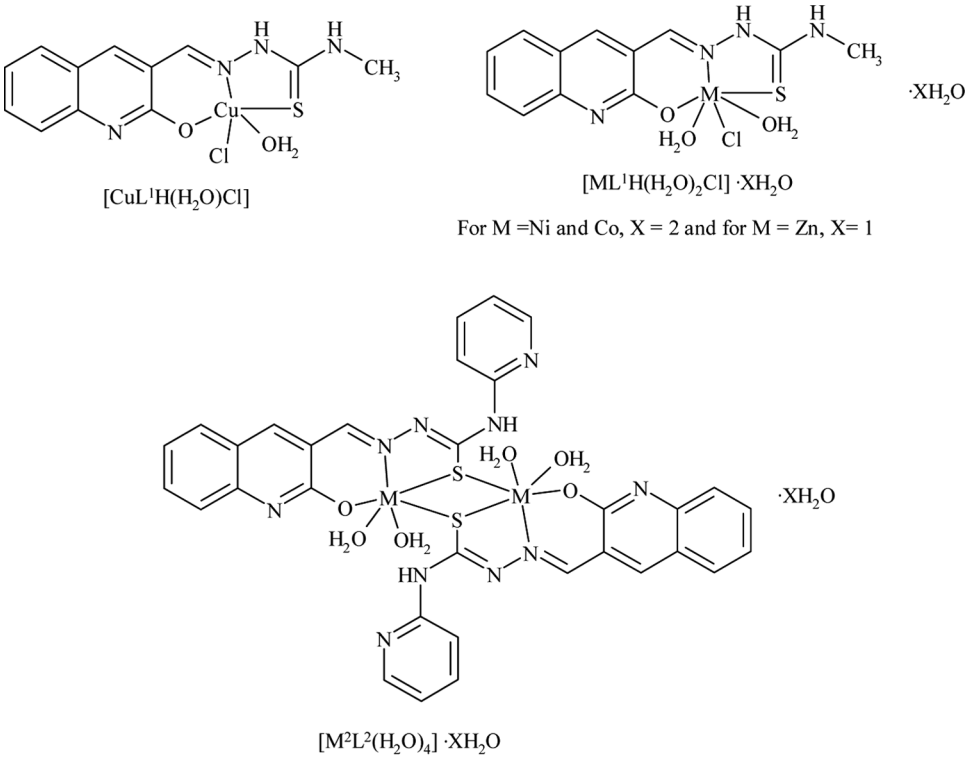

FIGURE 3 **Tentative structures assigned for the complexes.**

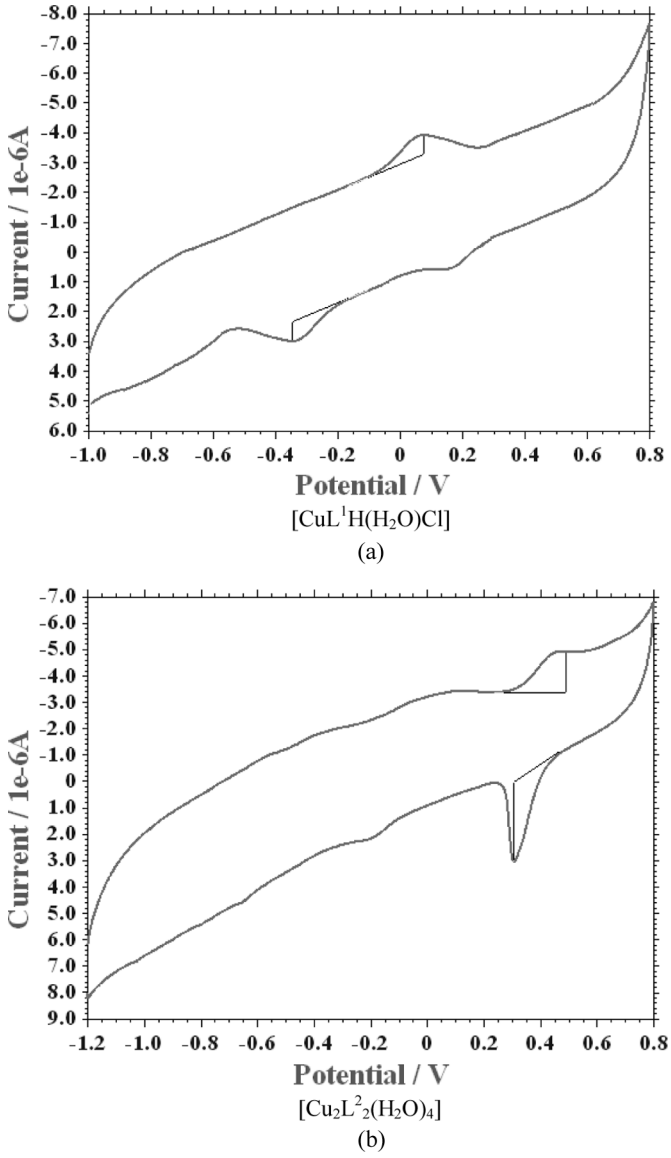

FIGURE 4 **Cyclic voltammograms of copper complexes with scan rate 0.1 V/s.**

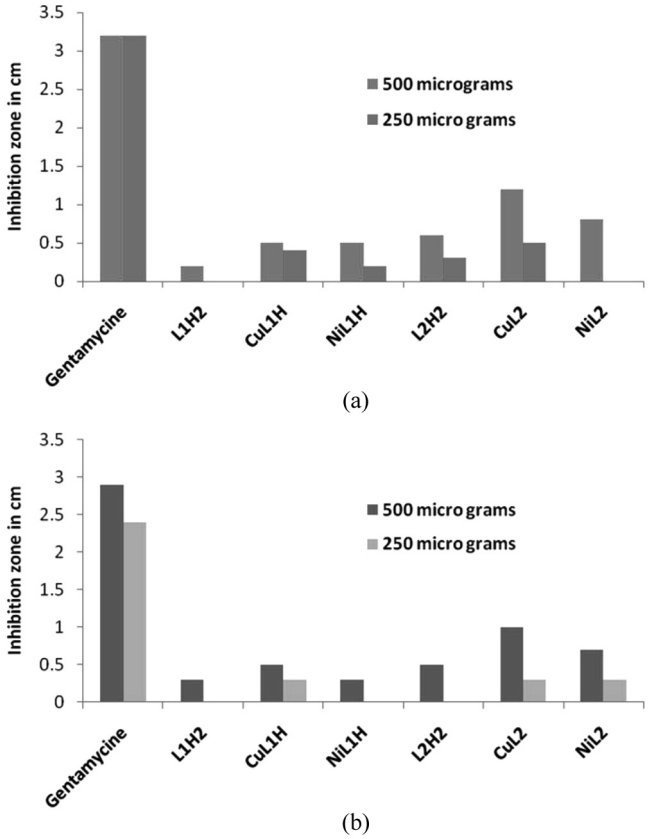

FIGURE 5 **Graphical representation of antibacterial analysis of the ligand and complexes. (a) *Escherichia coli*. (b) *Pseudomonas aeruginosa*.**

Figs. 5 and 6. From the data it is concluded that the ligand L^1H_2 is inactive against fungus *Cladosporidium*, less active against fungus *Aspergillus niger* and both the bacteria. The ligand L^2H_2 shows a high degree of inhibition against both bacteria and moderate activity against both the fungi. The observations made reveal that there is enhancement in the antimicrobial activity of the complexes, which is represented by the high degree of activity of copper and nickel complexes compared with their ligands. Enhancement in the antimicrobial property of thiosemicarbazones is often related to lipophilicity, which controls the rate of entry of molecules into the cell. The lipophilicity can be modified by the coordination, so that metal complexes become more accessible to the microbes, and hence the inhibitory action

TABLE 5 **Cyclic Voltammetry Results**

Complex	Scan rate (V/S)	E_{pa} (V)	E_{pc} (V)	ΔE_p (V)	$E_{1/2}$ (V)	I_{pc}/I_{pa}
$[CuL^1H(H_2O)Cl]$	0.15	0.13	0.23 & −0.28	0.11	0.18	1.08
	0.1	0.12	0.20 & −0.25	0.08	0.16	1.10
	0.05	0.11	0.18 & −0.23	0.07	0.145	1.15
$[Cu_2L^2_2(H_2O)_4]$	0.15	0.46	0.32	0.14	0.39	1.30
	0.1	0.44	0.33	0.09	0.385	1.31
	0.05	0.43	0.35	0.08	0.39	1.36

$E_p = E_{pa} - E_{pc}$; $E_{1/2} = [E_{pc} + E_{pa}]/2$.

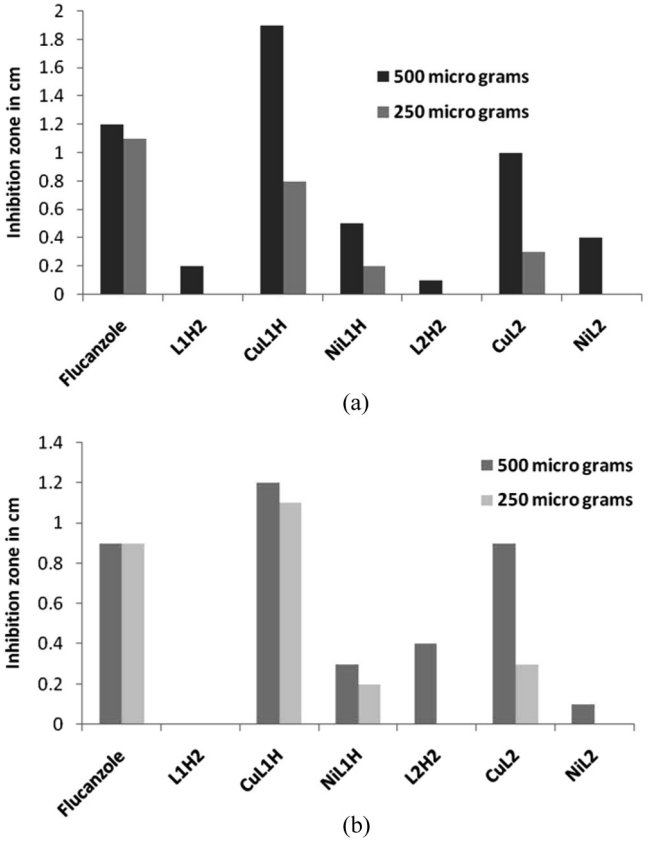

FIGURE 6 **Graphical representation of antifungal activity of ligand and complexes. (a) *Aspergillus niger*. (b) *Cladosporidium*.**

will be more.[22] Further, the complexation with the metal protects the molecule against enzymatic degradation, because of the inertness of certain metal ligand linkages; therefore, the activity can be reinforced by the combined effect of the ligand and metal residue.[23] Studies on the structural and kinetic properties involved in biological activity of an antitumor drug, cisplatin, reveals that the mechanism of action can involve binding to the metal *in vivo*, or the metal complex may be a vehicle for activation of the ligand as the inhibitory agent.[24] Moreover, coordination may lead to a significant reduction of drug resistance of a cell[25] and enhance the activity of drug.

CONCLUSION

The ligand L^1H_2 acts as tridentate monobasic and provides the square pyramidal geometry for the Cu(II) complex, whereas the Co(II), Ni(II), and Zn(II) complexes have an octahedral geometry. The ligand L^2H_2 behaves as tridentate dibasic in nature and forms octahedral complexes with all the metal ions. The ligand-to-metal ratio is found to be 1:1 and 2:2 for the complexes of L^1H_2 and L^2H_2, respectively. All the complexes are soluble in DMSO/DMF and are nonelectrolytic in nature. Only the copper complexes were found to be electrochemically active, exhibiting the quasireversible redox process. By considering the high antimicrobial property of the quinoline derivatives and bioaccessibility of Cu and Ni ions, the ligands and their respective copper and nickel complexes were screened against bacteria *Escherichia coli* and *Pseudomonas aeruginosa* and fungi *Aspergillus niger* and *Cladosporidium*. The compounds were found to exhibit higher activity against fungi than the bacteria. The complexes $[CuL^1H(H_2O)Cl]$ and $[Cu_2L^2_2(H_2O)_4]$ exhibited prominent activity toward *Aspergillus niger*, hence proving their usefulness in the field of biology as antimicrobial agents. Further, the investigation of the effectiveness of these compounds toward tumor cells is in progress.

ACKNOWLEDGMENTS

The authors thank the Department of Chemistry and USIC, Karnatak University, Dharwad, for providing spectral and analytical facilities. Recording of FAB mass spectra (CDRI Lucknow) and ESR spectra (IIT Bombay) are gratefully acknowledged. The authors (NVK and SMP) thank Karnatak University, Dharwad, for providing the Nilekani and University Research Scholarship and SB thanks the University Grant Commission for providing RFSMS.

REFERENCES

1. Raper, E. S. Complexes of heterocyclic thionates. Part 1. Complexes of monodentate and chelating ligands. *Coord. Chem. Rev.* **1996**, *153*, 199–255.
2. Quiroga, C.; Ranninger, C. N. Contribution to the SAR field of metallated and coordination complexes: studies of the palladium and platinum derivatives with selected thiosemicarbazones as antitumoral drugs. *Coord. Chem. Rev.* **2004**, *248*, 119–133.
3. Saha, D. K.; Padhye, S. B.; Sinn, E.; Newton, C. Synthesis, structure, spectroscopy and antitumor activity of hydroxy naphthoquinone thiosemicarbazone and its metal complexes against MCF-7 human breast cancer cell line. *Indian J. Chem. Inorg. Phys. Theor. Anal. Chem.* **2002**, *41A*, 279–283.
4. Cowley, A. R.; Dilworth, J. R.; Donnelly, P. S.; White, J. M. Copper complexes of thiosemicarbazone-pyridylhydrazine (THYNIC) hybrid ligands: A new versatile potential bifunctional chelator for copper radiopharmaceuticals. *Inorg. Chem.* **2006**, *45*, 496–498.
5. Gomez-Saiz, P.; Garcia-Tojal, J.; Maestro, M.; Mahia, J.; Lezama, L.; Rojo, T. Coordination modes in a (thiosemicarbazone)copper(II)/oxalato system—structures of $[Cu(L)]_2(ox)] \cdot 2H_2O$, $[Cu(HL)(ox)(H_2O)]$, $[\{Cu(HL)\}_2(ox)][Cu(ox)_2] \cdot 2H_2O$ and $[\{Cu(HL)\}_2(ox)](NO_3)_2$—ferro vs.

antiferromagnetic behavior in dinuclear compounds. *Eur. J. Inorg. Chem.* **2003**, 2123–2132.
6. Demertzi, D. K.; Domopoulou, A.; Demertzis, M. A.; Valle, G.; Papageorgiou, A. J. Palladium(II) complexes of 2-acetylpyridine N(4)-methyl, N(4)-ethyl and N(4)-phenyl-thiosemicarbazones. Crystal structure of chloro(2-acetylpyridine N(4)-methylthiosemicarbazonato) palladium(II). Synthesis, spectral studies, *in vitro* and *in vivo* antitumour activity. *J. Inorg. Biochem.* **1997**, *68*, 147–155.
7. Chen, Y. L.; Fang, K. C.; Shen, J. Y.; Hsu, S. L.; Tzeng, C. C. Synthesis and antibacterial evaluation of certain quinolone derivatives. *J. Med. Chem.* **2001**, *44*, 2374–2377.
8. Papageorgion, C.; Matt, A. V.; Joergensen, J.; Anderson, E.; Wagner, K.; Beerli, C.; Than, T.; Borex, X.; Florineth, A.; Rihs, S.; Schreier, M. H.; Weckbecker, G.; Hausser, C. Aromatic quinolinecarboxamides as selective, orally active antibody production inhibitors for prevention of acute xenograft rejection. *J. Med. Chem.* **2001**, *44*, 1986–1992.
9. Shinkai, H.; Ito, T.; Ida, T.; Kitao, Y.; Yamadu, H.; Uchida, I. 4-Aminoquinolines: Novel nociceptin antagonists with analgesic activity. *J. Med. Chem.* **2000**, *43*, 4667–4677.
10. Kaschula, C. H.; Egan, T. J.; Hunter, R.; Basilico, N.; Parapini, S.; Taramelli, D.; Pasini, E.; Monti, D. Structure-activity relationships in 4-aminoquinoline antiplasmodials. The role of the group at the 7-position. *J. Med. Chem.* **2002**, *45*, 3531–3539.
11. Joseph, B.; Darro, F.; Behard, A.; Lesur, B.; Collignon, F.; Decaestecker, C.; Frydman, A.; Guillaumet, G.; Kiss, R. 3-Aryl-2-quinolone derivatives: Synthesis and characterization of *in vitro* and *in vivo* antitumor effects with emphasis on a new therapeutical target connected with cell migration. *J. Med. Chem.* **2002**, *45*, 2543–2555.
12. Murugananthan, N.; Sivakumar, R.; Anbalagan, N.; Gunasekaran, V.; Leonard, J. T. Synthesis, anticonvulsant and antihypertensive activities of 8-substituted quinoline derivatives. *Biol. Pharm. Bull.* **2004**, *27*, 1683–1687.
13. Otto, M. C.; Narine, B.; Tarnowski, B. A. Versatile new synthesis of quinolines and related fused pyridines. Part 5. The synthesis of 2-chloroquinoline-3-carbaldehydes. *J. Chem. Soc. Perkin Trans.* **1981**, 1520–1530.
14. Sen, A. K.; Gupta, S. K. Possible antiamebic agents. XIX. Synthesis of 1,3,4-thiadiazolines and bi-1,3,4-thiadiazolines. *J. Ind. Chem. Soc.* **1962**, *39*, 628–634.
15. (a) Ali, O. A. M.; Khalil, M. M. H.; Attia, G. M.; Ramadan, M. R. Group VI dinuclear oxo metal complexes of salicylideneimine-2-anisole Schiff base. *Spectros. Lett.* **2003**, *36*, 71–82. (b) Lever, A. B. P. *Inorganic Electronic Spectroscopy*; Elsevier Publishing Company: NewYork, 1968.
16. Bailar, J. C.; Emeleus, H. J.; Nyholm, R.; Dickenson, A. F. T. *Comprehensive Inorganic Chemistry*; Oxford Pergamon Press: 1975.
17. Okawa, H.; Tadokoro, M.; Aratake, Y.; Ohba, M.; Shindo, K.; Mitsumi, M.; Tomono, M.; Funton, D. E. Dicopper(II,II) and dicopper (I,II) complexes of a series of dinucleating macrocycles. *J. Chem. Soc. Dalton Trans.* **1993**, 253–259.
18. (a) Mathews, S.; Kumari, S. B.; Rijulal, G.; Mohanan, K. Synthesis, characterization and antibacterial activity of some transition metal complexes of 2-N-(isatinamino)-3-carboxyethyl-4,5,6,7-tetrahydrobenzo[*b*]thiophene. *Sepctroscopy Letters*, **2008**, *41*, 154–161. (b) Seleem, H. S.; Shetary, B. A. E. L.; Khalil, S. M. E.; Mostafa, M.; Shebl, M. Structural diversity in copper(II) complexes of bis(thiosemicarbazone) and bis(semicarbazone) ligands. *J. Coord. Chem.* **2005**, *58*, 479–493.
19. Dutta, R. L.; Syamal, A. *Elements of Magneto Chemistry*, 2nd ed.; New Delhi, E. W. Press: 1993.
20. Martell, A. E.; Calvin, M. *Chemistry of the Metal Chelate Compounds*; Prentice Hall: New York, 1952.
21. Adsule, S.; Barve, V.; Chen, D.; Ahmed, F.; Dou, Q. P.; Padhye, S. B.; Sarkar, F. H. Novel Schiff base copper complexes of quinoline-2 carboxaldehyde as proteasome inhibitors in human prostate cancer cells. *J. Med. Chem.* **2006**, *49*, 7242–7246.
22. Farrell, N. Biomedical uses and applications of inorganic chemistry. *An overview. Coord. Chem. Rev.* **2002**, *232*, 1–4.
23. Weder, J. E.; Hambley, T. W.; Kennedy, B. J.; Lay, P. A.; MacLachlan, D.; Bramley, R.; Delfs, C. D.; Murray, K. S.; Moubaraki, B.; Warwick, B.; Biffin, J. R.; Regtop, H. L. Anti-inflammatory dinuclear copper(II) complexes with indomethacin. Synthesis, magnetism, and EPR spectroscopy. Crystal structure of the *n,n*-dimethylformamide adduct. *Inorg. Chem.* **1999**, *38*, 1736–1744.
24. Jamieson, E. R.; Lippard, S. J. Structure, recognition, and processing of cisplatin-DNA adducts. *Chem. Rev.* **1999**, *99*, 2467–2498.
25. West, D. X.; Padhye, S. B.; Sonawane, P. B. *Structural and Physical Correlations in the Biological Properties of Transition Metal Heterocyclic Thiosemicarbazone and Si>-Alkyldithiocarbazate Complexes. Structure and Bonding*; Springer Verlag: New York, 1991.